

Galactic Kinematics of Cepheids from Hipparcos Proper Motions [★]

Michael Feast ¹ and Patricia Whitelock ²

¹ *Astronomy Department, University of Cape Town, 7700 Rondebosch, South Africa.*

email: mwf@uctvax.uct.ac.za

² *South African Astronomical Observatory, PO Box 9, 7935 Observatory, South Africa.*

email: paw@sao.ac.za

21 September 2018

ABSTRACT

The Hipparcos proper motions of 220 galactic Cepheids, together with relevant ground-based photometry, have been analysed. The effects of galactic rotation are very clearly seen. Mean values of the Oort constants, $A = 14.82 \pm 0.84 \text{ km s}^{-1}\text{kpc}^{-1}$, and $B = -12.37 \pm 0.64 \text{ km s}^{-1}\text{kpc}^{-1}$, and of the angular velocity of circular rotation at the Sun, $\Omega_o = 27.19 \pm 0.87 \text{ km s}^{-1}\text{kpc}^{-1}$, are derived. Comparison of the value of A with values derived from recent radial velocity solutions confirm, within the errors, the zero-points of the PL and PLC relations derived directly from the Hipparcos trigonometrical parallaxes of the same stars. The proper motion results suggest that the galactic rotation curve is declining slowly at the solar distance from the galactic centre ($(d\Theta/dR)_o = -2.4 \pm 1.2 \text{ km s}^{-1}\text{kpc}^{-1}$). The component of the solar motion towards the North Galactic Pole is found to be $+7.61 \pm 0.64 \text{ km s}^{-1}$. Based on the increased distance scale deduced in the present paper the distance to the galactic centre derived in a previous radial velocity study is increased to $R_o = 8.5 \pm 0.5 \text{ kpc}$.

Key words: Cepheids - distance scale - Galaxy:fundamental parameters

1 INTRODUCTION

The measurement of trigonometrical parallaxes and proper motions of Cepheid variables by the Hipparcos satellite (ESA 1997) represents a major advance over earlier work because of the scope and accuracy of the new results and the fact that they are referred to a co-ordinate system which is uniform over the whole sky and based on the positions of distant extragalactic objects. The link between the Hipparcos reference frame and the International Celestial Reference System (ICRS) based on the positions of extragalactic radio sources implies that the Hipparcos proper motions are quasi-inertial to within $\pm 0.25 \text{ mas yr}^{-1}$ (ESA 1997 volume 1 section 1.2). In a previous paper (Feast & Catchpole 1997 = paper 1), the zero-point of the Cepheid period-luminosity (PL) relation was derived from Hipparcos trigonometrical parallaxes. The present paper is primarily concerned with an analysis of the Hipparcos proper motions. We also use the Hipparcos trigonometrical parallaxes to derive zero-points for PL and period-luminosity-colour (PLC) relations which have been recently adopted in discussions of the radial velocities of Galactic Cepheids. This allows us to revise Galactic

constants derived from the radial velocity studies. The constants of absolute and differential rotation of our Galaxy are derived from the Hipparcos proper motions. The value of the Oort constant of differential rotation, A , derived from the proper motions is essentially independent of the adopted distance scale; whilst that derived from radial velocities is nearly inversely proportional to this scale. Thus a comparison allows us to confirm the Cepheid luminosity scale derived from the trigonometrical parallaxes.

2 OBSERVATIONAL DATA

The Cepheids discussed in the present paper are listed in Table 1. This table gives the Hipparcos Catalogue number (HIP), the variable star name and the values of $\langle V \rangle$ and $\langle B \rangle - \langle V \rangle$ adopted. These latter values are from the sources discussed in paper 1. The table also gives the log of the period or, for the stars noted in paper 1 as pulsating in the first overtone, the log of the fundamental period calculated in the manner described there. These latter stars are denoted by “o” in the last column of the table. The effects of overtone, and possible overtone, pulsators on the trigonometrical parallax work were discussed in detail in paper 1

[★] Based on data from the Hipparcos astrometry satellite

so far as the 26 stars used for the adopted PL zero-point were concerned. Any likely effect on the PL zero-point of an uncertainty with regard to pulsation mode was shown to be very small and this also applies to the trigonometrical parallax analyses of the present paper. It remains possible that there are a limited number of unrecognised overtone pulsators amongst the full set of stars listed in Table 1. Most of our results from the proper motions (e.g. concerning A and Ω_o) are quite insensitive to distance errors and thus to a possible misidentification of the pulsation mode of some stars (see, e.g. sections 5 and 6 below). Second-order terms and values of the local solar motion will be affected by any such misidentification but the effect is likely to be very small. For instance the value of w_o (defined in section 9 below) might be slightly underestimated due to this cause.

In carrying out the analyses two slightly different sets of reddenings (E_{B-V}) have been used. When a PL relation has been used to estimate distances the reddenings were derived from the period-colour relation used in paper 1, viz;

$$B - V = 0.416 \log P + 0.314 \quad (1)$$

(Laney & Stobie 1994). The advantage of doing this is discussed in paper 1. However, this advantage no longer applies when the distances are being derived from a PLC relation. In that case the reddenings listed in Table 1 were used. These were taken where possible from the compilation of Caldwell & Coulson (1987) and are on the two-colour, BVI , system with a zero-point derived from Cepheids in open clusters. It should be noted that reddenings in the BVI system provide the basis for the PC relation (equation 1). For stars which are not in the Caldwell & Coulson compilation, reddenings were taken from Fernie (1990) or from determinations on the same system (Fernie et al. 1995, electronic catalogue). With the adopted reddenings, values of A_V were derived using equation 7 of paper 1 (see Laney & Stobie 1993).

The astrometric data can be obtained directly from the Hipparcos Catalogue (ESA 1997). This gives the trigonometrical parallaxes of the stars together with their standard errors. The parallaxes of the 26 Cepheids of highest weight in the PL zero-point solution of paper 1 are given in that paper. The Hipparcos Catalogue also gives for each star the proper motions in Right Ascension and Declination ($\mu_{\alpha*} = \mu_\alpha \cos \delta$ and μ_δ), their standard errors and the coefficient of correlation between the two proper motion components. All the astrometric data are expressed in milli-arcsec (mas).

3 PLC AND PL ZERO-POINTS

When in later sections of this paper the results from the Hipparcos proper motions are compared with radial velocity studies we shall be referring principally to two recent radial velocity studies of Cepheid kinematics, viz., Metzger et al. (1997 = MCS) and Pont et al. (1994 = PMB). In deriving distances MCS use a PL relation whilst PMB use a PLC relation. The Hipparcos trigonometrical parallaxes are used below to derive zero-points of these relations. A comparison with the zero-points actually used by MCS and PMB then indicates the scaling factor necessary to bring their results onto the scale set by the trigonometrical parallaxes.

MCS use a PL relation of the form:

$$\langle M_V \rangle = -2.87 \log P + \rho_1 \quad (2)$$

with $\rho_1 = -1.23$. Revised values of ρ_1 have been derived using precisely the same methods and data as used to derive the PL relation in paper 1 and for the same groupings of stars. Four solutions are given in Table 2. They correspond to solution A and numbers 1, 2, 4 and 6 of paper 1 Table 2. In paper 1 additional solutions (solutions B) were given taking into account possible errors in addition to those of the parallaxes. Since these were shown there to be only marginally different from solutions A they are not given in the present case. As with the analogous solution in paper 1 we adopt solution 4 as the best value of ρ_1 ($= -1.38 \pm 0.09$). Thus the Hipparcos parallaxes indicate that the MCS zero-point should be brightened by 0.15 mag or their distance scale increased by 7 percent. It may be noted that the interstellar reddenings adopted by MCS are on the BVI system of Caldwell & Coulson (1987). As with those adopted in paper 1 they have as their zero-point the reddenings of Cepheids in open clusters. Thus these two systems of reddening should be closely similar.

PMB use a PLC relation of the form:

$$\langle M_V \rangle = -3.80 \log P + 2.70(\langle B \rangle - \langle V \rangle)_0 + \rho_2 \quad (3)$$

(see Feast & Walker 1987). PMB adopt $\rho_2 = -2.27$. In deriving a value of ρ_2 from the Hipparcos trigonometrical parallaxes, the general procedure of paper 1 was again followed. But for the reasons given in section 2 (above), the reddenings listed in Table 1 were used. For the 26 stars of highest weight (which are the same 26 stars listed in Table 1 of paper 1) all the reddenings come directly from Caldwell & Coulson (1987).

There should be negligible intrinsic scatter in the PLC relation. Martin et al. (1979) (see also Feast & Walker 1987) found that a sample of LMC Cepheids showed a scatter of 0.14 ± 0.02 about a PLC relation. This scatter includes observational error, errors in reddening corrections and distance scatter within the LMC. It should therefore be an upper limit to the scatter in the sample of stars used with the Hipparcos parallaxes, especially since these are brighter and generally more extensively observed photometrically. Note that because the coefficient of the colour term in the PLC relation is similar to the ratio A_V/E_{B-V} , the PLC relation is relatively insensitive to errors in the reddenings. Following the method discussed in paper 1, the PLC zero-point was derived taking into account the errors in the parallaxes and the possible scatter in the PLC relation. Table 3 shows the results with this latter scatter (σ_{PLC}) taken as 0, 0.10, or 0.20 mag. The solutions correspond to the four solutions of Table 2. It is clear that within reasonable limits the value of σ_{PLC} has little effect. We adopt solution 4 with $\sigma_{PLC} = 0.10$ (-2.38 ± 0.10). This is 0.11 mag brighter than the zero-point used by PMB, or an increase in the distance scale of 5 percent.

4 THE ADOPTED PROPER MOTIONS

The Hipparcos proper motions and their errors (see section 2 above) were converted into components in galactic longitude and latitude ($\mu_{\ell*} = \mu_\ell \cos b$, and μ_b) and their errors, using the constants provided in the Hipparcos Catalogue and taking into account the correlation between proper motions in Right Ascension and Declination. Then if μ is the proper

motion in mas and d is the distance in kpc, the corresponding velocity is $\kappa\mu d$ km s⁻¹ where $\kappa = 4.74047$ (a value also taken from the Hipparcos Catalogue).

In analysing the proper motions account must be taken in the weighting not only of the standard errors of the proper motion components themselves ($\sigma_{\ell^*}, \sigma_b$) but also the scatter about an adopted galactic model due to the random motions of the stars. The weights were taken as proportional to the reciprocals of the squares of $\sigma_{\kappa\mu\ell^*}$ and $\sigma_{\kappa\mu b}$, where,

$$\sigma_{\kappa\mu\ell^*}^2 = (\kappa\sigma_{\ell^*})^2 + (\alpha^2 \sin^2 l + \beta^2 \cos^2 l)/d^2 \quad (4)$$

and

$$\sigma_{\kappa\mu b}^2 = (\kappa\sigma_b)^2 + (\alpha^2 \cos^2 \ell \sin^2 b + \beta^2 \sin^2 \ell \sin^2 b + \gamma^2 \cos^2 b)/d^2. \quad (5)$$

α, β and γ are the axes of the velocity ellipsoid for which we have adopted the values 13, 9 and 5 km s⁻¹ for Cepheids from Delhaye (1965)(see also PMB).

Of the Cepheids for which astrometric data were available from Hipparcos, the following stars have been omitted in the analyses for the reasons given below. In most cases the stars were rejected because of the large peculiar velocities (given below) derived in preliminary analyses using PL distances and the proper motions. H10, H29 and H30 indicate an anomalous entry in the relevant field, Hn, of the Hipparcos catalogue (for more details see the explanatory supplement). In the following H10 indicates that the star is flagged in H10 as being in a binary or multiple system; H29 indicates that 20 percent or more of the data were rejected in the astrometric solution and H30 indicates that the goodness of fit statistic is greater than 3, possibly implying a poor astrometric solution.

DP Vel; HIP 46610; Photometry too sparse; see paper 1.

AW Per; HIP 22275; Binary; see paper 1.

AX Cir; HIP 72773; Binary; see paper 1; H10, H30.

UX Per; HIP 10332; Peculiar velocity ~ 500 km s⁻¹; H10, H29, H30.

SS CMa; HIP 36088; Peculiar velocity ~ 200 km s⁻¹.

V Vel; HIP 45949; Rejected by PMB due to discrepant radial velocity. Rejected by Caldwell & Coulson (1987) due to discrepant colours. Peculiar velocity ~ 80 km s⁻¹.

SU Cru; HIP 59996; Rejected by PMB due to discrepant radial velocity. Peculiar velocity ~ 240 km s⁻¹; H10, H29.

SY Nor; HIP 77913; Peculiar velocity ~ 100 km s⁻¹; H10, H30.

TW Nor; HIP 78771; Peculiar velocity ~ 100 km s⁻¹. This is an important star in, or in the direction of, the open cluster Lynga 6. Caldwell & Coulson (1987) rejected it as a PL calibrator because it gave a discrepant zero-point but more recently Laney & Stobie (1994) have included it in a zero-point determination by the cluster method.

5 FIRST ORDER SOLUTION FOR GALACTIC ROTATION

It is useful to begin with a simple, first order (“Oort” type) solution for galactic rotation from the proper motions. The relevant equation is generally written in the form;

$$\kappa\mu_{\ell^*} = (u_o \sin \ell - v_o \cos \ell)/d + (A \cos 2l + B) \cos b, \quad (6)$$

where u_o and v_o are the components of the local solar motion (with respect to young objects) towards the galactic centre and in the direction of galactic rotation. The Oort constants are defined by

$$A = -\frac{1}{2}R_o(d\Omega/dR)_o \quad (7)$$

and

$$B = -\Omega_o - \frac{1}{2}R_o(d\Omega/dR)_o, \quad (8)$$

where R is the distance of the star from the galactic centre and Ω the angular velocity ($=\Theta/R$, Θ being the circular velocity). Subscript “o” indicates the values of these quantities at the solar position. However, the quantity of interest is often not B itself but

$$A - B = \Omega_o = \Theta_o/R_o. \quad (9)$$

It is useful therefore to solve equation 6 in the form:

$$\kappa\mu_{\ell^*} = (u_o \sin \ell - v_o \cos \ell)/d + (2A \cos^2 \ell - \Omega_o) \cos b. \quad (10)$$

Thus here and in the rest of the paper we work in terms of A and Ω_o , but explicit values of B are given for our final solutions. Because of the uniformity of the Hipparcos reference frame and the fact that it is tied to the positions of extragalactic objects, the values of B and Ω_o (which are directly affected by any rotation of the reference frame) should be considerably more reliable than previous values.

There have been a large number of determinations from radial velocities of the components of the local solar motion from Cepheids. These stars are expected in the mean to be in circular rotation about the Galactic Centre. There is some discussion of the local solar motion, relative to extreme population I objects, in section 9, below. We adopt in this section either $u_o = 9$ and $v_o = 13$ km s⁻¹ or $u_o = 9.32$ and $v_o = 11.18$ km s⁻¹. The latter is from PMB. Table 4 shows a number of solutions for A and Ω_o . Except in the case of solution 3, the distances used in these solutions were obtained with the PL relation derived in paper 1 from the Hipparcos trigonometrical parallaxes, viz.

$$\langle M_V \rangle = -2.81 \log P - 1.43, \quad (11)$$

together with reddenings obtained from equation 1 above. For solution 3 the “PLC” distances discussed in section 3 were used. Solution 4 shows the effect of decreasing all distance moduli by 0.4 mag. In solutions 5 and 6 the data are divided into two groups on the basis of the stellar distance, and in solution 7 the effect of forcing $2A$ to equal Ω_o , as is required for a flat rotation curve ($\Theta = \text{constant}$), is shown.

These various solutions show that the derived constants are rather insensitive to the adopted distance scale. There is a suggestion that the derived value of A increases with distance (though the increase is within the errors). This may be due both to local streaming motions and (for the more distant stars) to the neglect of higher-order terms in the equation used (equation 10). Forcing a flat rotation curve on the data leads to a distinctly smaller value of A (13.34 ± 0.42) than that derived from the other solutions.

Figure 1 shows a plot of the distances of Cepheids with Hipparcos proper motions projected onto the Galactic Plane (PL distances). Whilst many previous studies of galactic rotation from proper motions have referred to a relatively

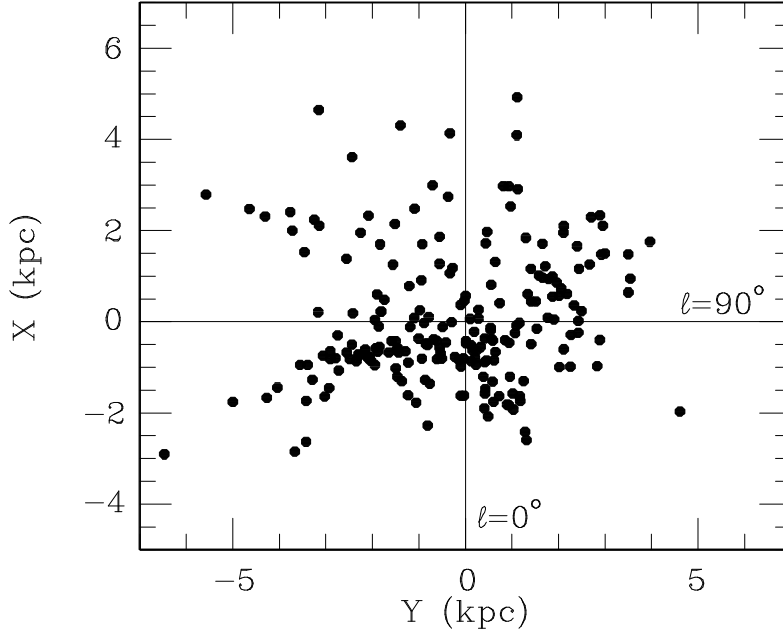


Figure 1. The distribution of the Cepheids used in the proper motion solutions seen projected onto the galactic plane. The Sun is at the origin of the co-ordinate system. The distances are from the PL relation derived in paper 1.

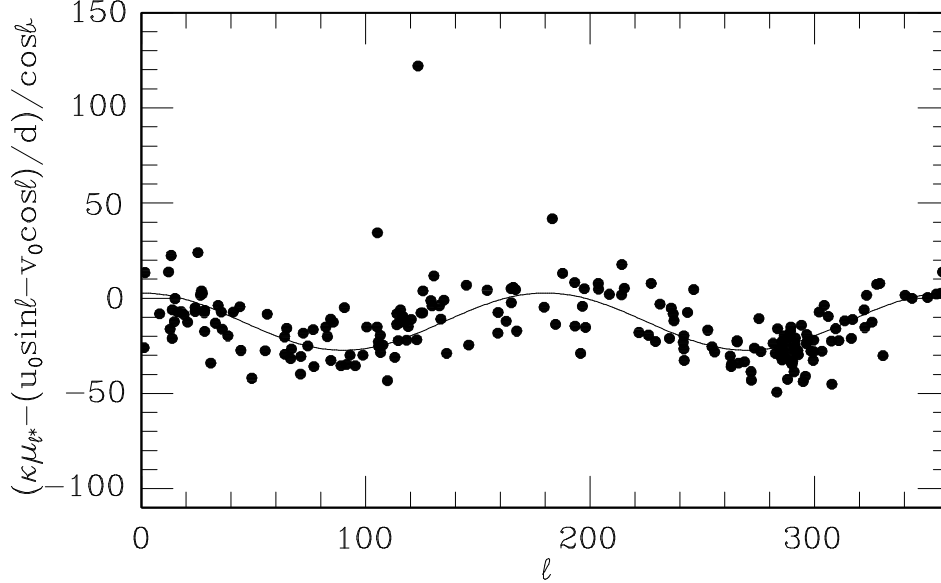


Figure 2. The proper motion in galactic longitude multiplied by κ , and corrected for local solar motion, plotted against galactic longitude. The curve corresponds to solution 2 of Table 4. The three outstanding stars are nearby and have low weight in the solution (see text for further details).

small region around the sun, the Hipparcos data covers a significant region of the Galactic Disc.

The quantity $(\kappa\mu_{\ell^*} - (u_0 \sin \ell - v_0 \cos \ell)/d) / \cos b$ is shown in Fig 2 plotted against galactic longitude (ℓ) for solution 2 of Table 4. Figures 3 and 4 show similar plots for the nearer and more distant stars (solutions 5 and 6), the

curves in each case illustrate the corresponding solutions in Table 4.

Whilst the effect of Galactic rotation on proper motions has long been known (e.g. Oort 1927), it does not seem to have been possible prior to the Hipparcos results to demonstrate this from plots of proper motions for individual stars

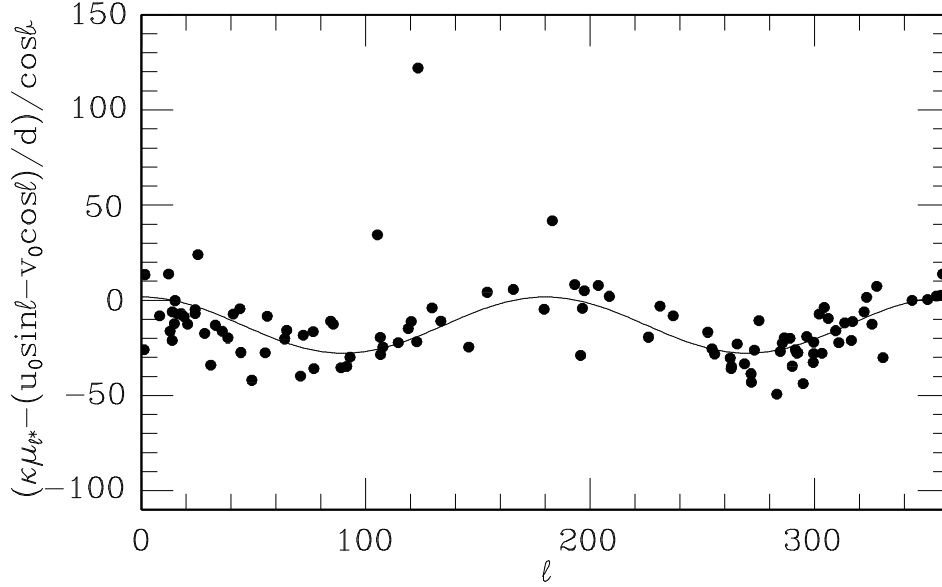


Figure 3. As Fig 2 but for stars with distances less than 2 kpc. The curve illustrates solution 5 of Table 4.

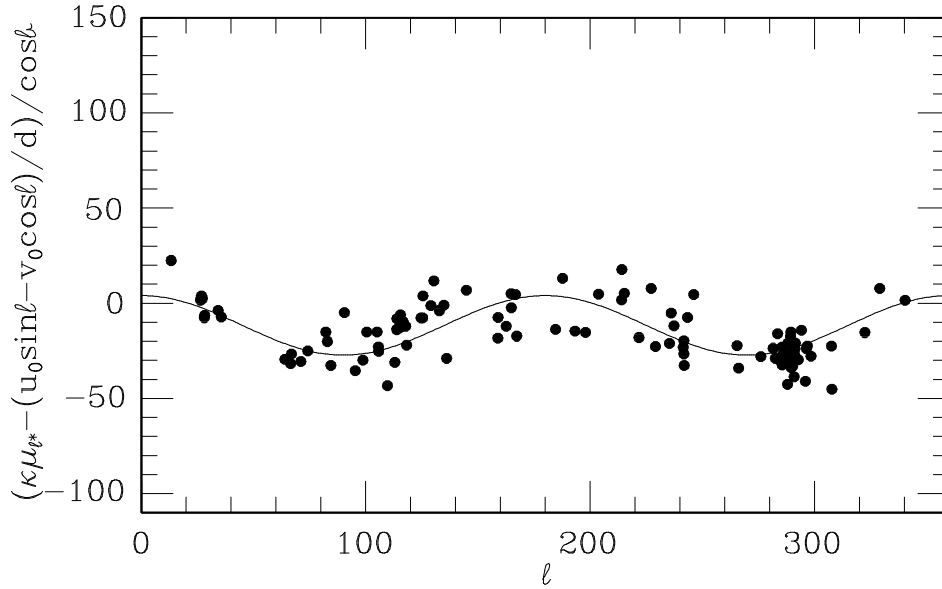


Figure 4. As Fig 2 but for stars with distances equal to or greater than 2 kpc. The curve illustrates solution 6 of Table 4.

in the way shown in Figs 2, 3 and 4. Note that the three stars which lie conspicuous above the others in Figs 2 and 3 are α UMi, δ Cep and RT Aur. These stars are sufficiently close to the sun that their peculiar velocities have a large effect on their proper motions. Their deviations from the mean curve can be accounted for by quite modest peculiar velocities (10 to 20 km s⁻¹). In view of the weighting sys-

tem adopted, they have little effect on the derived galactic rotation parameters.

6 GALACTIC ROTATION INCLUDING HIGHER ORDER TERMS. I

In this and the next section we discuss the results obtained when higher order terms are introduced into the Galactic ro-

tation formulae. The present section adopts the formulation used by PMB in their analysis of Cepheid radial velocities. This involves retaining terms in d/R_o and also higher derivatives of Θ . Thus to the level of approximation adopted by PMB the relation in Galactic longitude becomes;

$$\kappa\mu_{\ell*} = (u_o \sin \ell - v_o \cos \ell)/d - \Omega_o \cos b + \left[\frac{R_p}{d} \cos \ell - \cos b \right] \\ \times \left[\frac{2AR_o}{R} (1 - R/R_o) + \frac{(R-R_o)^2}{2R} \Theta'' + \frac{(R-R_o)^3}{6R} \Theta''' \right] \quad (12)$$

where, $\Theta'' = d^2\Theta/dR^2$ and $\Theta''' = d^3\Theta/dR^3$.

We have not attempted to derive a value of R_o from the proper motions but have adopted a value from PMB either directly or adjusted to the Hipparcos parallax distance scale (section 3) by using fig 5 of PMB.

Table 5 gives the results of various analyses. Solution 1 is the radial velocity solution adopted by PMB. It should be noticed that the errors given in this case are ‘‘internal’’ errors and do not include any uncertainty in the distance scale adopted by PMB. For instance if their PLC zero-point is uncertain by 0.1 mag then the rms error of their derived value of A is $0.7 \text{ km s}^{-1} \text{ kpc}^{-1}$ due to this cause alone. Solution 2 shows the effect on some of these constants of increasing all the PMB distance moduli by 0.2 mag. These results were derived from fig 5 of PMB. The remaining solutions are from the proper motion data. For solutions 3 to 13 the adopted distances were derived from the PL relation obtained from the Hipparcos trigonometrical parallaxes in paper 1 together with the PC relation adopted there. In solutions 14 to 19 the distances were determined from the PLC relation derived in section 3 above together with the reddenings discussed there.

In several of the proper motion solutions the values of u_o and v_o were fixed at the values derived by PMB (solution 1). Similarly in some solutions the values of R_o , Θ'' and Θ''' were fixed as the values from solutions 1 or 2, or Θ'' and Θ''' were taken as zero. Solution 3 in which only R_o was fixed yields values of Θ'' and Θ''' which are of opposite sign to the values obtained from the radial velocities. However, the value of v_o which goes with this solution is anomalous (much larger than expected for young objects). If the local solar motion is fixed at the PMB value (solution 4) the values of Θ'' and Θ''' do not differ significantly from zero. When the values of R_o , Θ'' and Θ''' are fixed at the various values discussed above the values of the local solar motion derived are close to expected values for young objects (see Table 7 section 9), e.g. solutions 5, 7 and 9. The value of A obtained (solution 11) when a flat rotation curve is assumed is significantly lower than other values. This is discussed further in section 7. The value of Ω_o is evidently rather insensitive to the precise method of solution.

To the extent that the proper motion results have failed to confirm the values of Θ'' and Θ''' derived from radial velocities by PMB, there must be a question as to whether the values for these quantities given by PMB are of general significance for the Galaxy or simply the effects of random or group motions (including streaming along spiral arms) of the sample of objects they studied. Nevertheless, in comparing the values of A determined from proper motions and from radial velocities it seemed best to fix the values of u_o , v_o , R_o , Θ'' and Θ''' from the radial velocity solutions, although setting the last two quantities to zero yields negligibly different results. For our final solution (solution 19 of Table 5) we adopt $R_o = 8.5 \text{ kpc}$ (see below) and corresponding values

of Θ'' and Θ''' from fig 5 of PMB together with the values of u_o and v_o from PMB.

Thus we adopt from the proper motions

$$A = 14.82 \pm 0.84 \text{ km s}^{-1}, \quad B = -12.37 \pm 0.64 \text{ km s}^{-1} \quad \text{and} \\ \Omega_o = 27.19 \pm 0.87 \text{ km s}^{-1}.$$

These results are essentially independent of the adopted distance scale or of scaling the PMB values of R_o , Θ'' and Θ''' (compare solutions 15, 17 and 19 of table 5). Comparison of this adopted value of A with the value from radial velocities (15.92 ± 0.34) leads (via fig 5 of PMB) to a revised zero-point of the PLC relation (equation 3) of

$$\rho_2 = -2.43 \pm 0.13$$

However, the reddenings adopted by PMB differ slightly in the mean from those in Table 1 and this must be taken into account in comparing the value of ρ_2 derived from proper motions and radial velocities with that derived in section 3 directly from the trigonometrical parallaxes. The reddening difference is $\Delta E_{B-V} = 0.011 \pm 0.003$ (from 194 Cepheids in common) with the reddenings of PMB being greater. Taking this difference into account we obtain;

$$\rho_2 = -2.42 \pm 0.13$$

which agrees closely with the value derived from the trigonometrical parallaxes, viz;

$$\rho_2 = -2.38 \pm 0.10.$$

Whilst this forms a very useful check on the distance scale derived from the Hipparcos trigonometrical parallaxes, it should be realised that any statistical parallax determination is dependent on the model adopted for galactic motions and therefore does not have the fundamental status of the trigonometrical parallaxes.

PMB derive $R_o = 8.09 \pm 0.30 \text{ kpc}$ from radial velocities, where the quoted error does not take into account uncertainties in their adopted distance scale. This may be revised using the Hipparcos trigonometrical parallax zero-point and accounting for the difference in reddening systems. One then obtains (using fig 5 of PMB),

$$R_o = 8.5 \pm 0.5 \text{ kpc},$$

where the standard error now takes into account the uncertainty in the PLC zero-point.

7 GALACTIC ROTATION INCLUDING HIGHER ORDER TERMS. II

In a recent paper Metzger et al. (1997 =MCS) have re-investigated the galactic kinematics of Cepheids from radial velocities and have in particular found some evidence for a weak ellipticity of the galactic disc. The zero-point of their adopted PL relation was re-evaluated in section 3 above. In the approximation adopted by MCS, which includes the assumption that the rotational velocity (Θ) is constant, so that, $\Theta_o = 2AR_o$, the proper motions in galactic longitude should be given by the following expression

$$\kappa\mu_{\ell*} = (u_o \sin \ell - v_o \cos \ell)/d \\ - \Omega_o [(1 - R_o/R) R_o \cos \ell/d + R_o \cos b/R] \\ + f [R_o \sin(2\phi + l)/dR - \sin 2\phi \cos b/R - \sin \ell/d] \quad (13)$$

where

$$\sin \phi = d \cos b \sin \ell / R \quad (14)$$

and f is a constant equal to $\Theta_o s(R_o)$. $s(R_o)$ is the galactic ellipticity term as defined by MCS. The radial velocity solu-

tions of MCS lead to $f = +10.2 \pm 3.8 \text{ km s}^{-1}$. A variety of solutions have been carried out using the Hipparcos proper motions to solve equation 13. These include adopting values for u_o and v_o from the radial velocity solutions of PMB (see previous section) and MCS (9.30 and 13.50 km s^{-1}). The results are shown in Table 6 where the first solution is the radial velocity solution adopted by MCS. In carrying out these analyses distances have been determined using the PL and PC relations discussed in paper 1. As indicated above the reddening corrections adopted by MCS should be on a system close to this. In no case did the proper motion solutions yield a value for f which was significantly different from zero. The errors of f from proper motions are comparable with those in the MCS radial velocity work. This leaves open the possibility that the positive value of f found by MCS might reflect group motions, including flows along spiral arms, rather than a general ellipticity of the galactic disc. It is worth noticing that in a recent paper on Cepheid radial velocities Pont et al. (1997) find no significant evidence for non-axisymmetric components in the rotation of the outer galactic disc.

As in the case of the solutions of the previous section the value of Ω_o is quite insensitive to variations in the various other parameters of the solutions. If we adopt solution 6 in which R_o , u_o , v_o and f are fixed at the values adopted by MCS then $\Omega_o = 26.80 \pm 0.83 \text{ km s}^{-1}\text{kpc}^{-1}$ and thus $A = 13.40 \pm 0.42 \text{ km s}^{-1}\text{kpc}^{-1}$.

The value of A derived from radial velocities scales inversely with the distance scale (or very nearly so). Thus the value derived by MCS from radial velocities (15.47 ± 1.2 , note that this error is from the two errors quoted by MCS in quadrature) together with the value just derived from proper motions, indicates that the MCS scale is underestimated by 0.31 ± 0.19 mag. Whilst this estimate agrees within the errors with that derived from the parallaxes in section 3 (0.15 ± 0.09 mag) it cannot be regarded with particular confidence. Reference to sections 5 and 6 shows that when the rotation curve is assumed flat the value of A derived from the proper motions is smaller than when the rotation curve is not so constrained. This clearly illustrates that the model adopted in deriving distance scales from proper motions and radial velocities may have a significant effect on the derived result. In this particular case the problem probably arises because the assumption of a flat rotation curve only affects second and higher order terms in the radial velocity solutions, but affects the proper motion solutions in the first order terms.

MCS derive a value of $R_o = 7.66 \pm 0.54 \text{ kpc}$ (combining their two quoted error estimates). The quoted error allows for uncertainty in their adopted distance scale. The PL zero-point (section 3) from the trigonometrical parallaxes scales this result to $8.2 \pm 0.6 \text{ kpc}$. As MCS point out the value of R_o that they derive is sensitive to the galactic ellipticity term. If this is set equal to zero a further increase in R_o of about 4 percent is necessary which would bring their value to about 8.5 kpc , i.e. to the value derived above from the PMB work.

8 AN ESTIMATE OF Θ'_o AND THE DISTRIBUTION OF VELOCITY RESIDUALS

Tables 4, 5, and 6 show that, apart from the solutions in which Ω_o was constrained to equal $2A$, the former is always less than the latter. Since,

$$\Theta'_o = (d\Theta/dR)_o = \Omega_o - 2A \quad (15)$$

this indicates that in the mean the rotation curve is declining over the region covered by the Cepheid proper motions. Taking into account the covariance of Ω_o and A in the various solutions the values of Θ'_o are $-2.8 \pm 1.3 \text{ km s}^{-1}\text{kpc}^{-1}$ for the first order solution (Table 4 solution 2) and -2.4 ± 1.2 for solution 19 of Table 5. This is thus a $2\text{-}\sigma$ result. Evidence for a declining rotation curve at the Sun's distance from the Galactic Centre is strengthened if we accept the radial velocity result (PMB, see section 6 above) that Θ''_o is also negative.

As Fig 1 shows, the Cepheids in the Hipparcos sample cover a range in R from about 6 kpc to 12 kpc (adopting $R_o = 8.5 \text{ kpc}$). There is other evidence for a declining rotation curve over this range of galactocentric distances. For instance Brand & Blitz (1993) derived a rotation curve from radial velocities of HII regions which shows a similar effect. Their fig 5 suggests a somewhat more negative value of Θ'_o than the one derived from Cepheid proper motions, but in view of the uncertainties the difference is probably not significant. Brand & Blitz fit a gradually rising rotation curve to their complete data set and attribute the declining portion to the effects of local streaming motions. The fact that the decline is seen in both the radial velocities and the proper motions which sample the velocity field in different ways, must strengthen the view that the decline is a major kinematic feature of this region of the Galaxy. It should also be noted that Binney & Dehnen (1997) have argued that the rise seen in the Brand-Blitz rotation curve for $R > 12 \text{ kpc}$ may be an artifact of the spatial distribution of objects in the Brand-Blitz sample and that the rotation curve may in fact continue to decline in the outer regions of the Galaxy. More recently Pont et al. (1997) have given evidence from radial velocities of Cepheids in the outer galactic disc that the rotation curve declines, at least initially, beyond the solar distance from the Centre.

Figure 5 shows the residual velocities of the Cepheids in galactic longitude as seen projected on the Galactic Plane. These were derived from the proper motions adopting solution 19 of Table 5. It should be borne in mind that on the average the uncertainty in these velocity residuals increases with distance (since they are derived from proper motions). It has long been known that the radial velocity residuals for young objects (OB stars, Cepheids) are not randomly distributed but tend to show clumping on a scale of order of a kiloparsec (Weaver 1964, Feast 1967) which may possibly be associated with spiral structure (Humphreys 1972). Recent radial velocity work on Cepheids continues to show evidence of such clumping (PMB, MCS). There is some slight suggestion of clumping of velocity residuals in Fig 5 (e.g. for distant stars in the anti-centre direction) but the evidence is not strong and there is no very obvious correlation of the velocity residuals from proper motions with those from radial velocities (e.g. fig 7 of PMB).

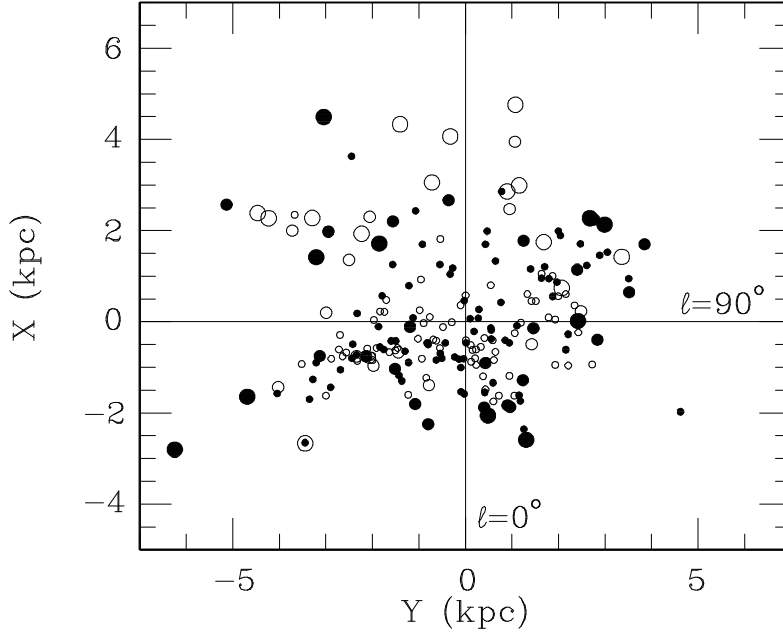


Figure 5. The velocity residuals derived from solution 19 of Table 5 for the proper motions in galactic longitude are shown plotted at their projected positions in the galactic plane. The size of the symbol indicates the size of the residual without regard to sign. Large circles, $> 40 \text{ km s}^{-1}$; medium circles, $20 - 40 \text{ km s}^{-1}$; small circles, $0 - 20 \text{ km s}^{-1}$. Filled circles are for positive residuals and open circles for negative residuals.

9 THE LOCAL SOLAR MOTION

A large number of determinations of the local solar motion relative to young objects have been made in the past. No attempt is made to review them all here. Table 7 contains the results of recent Cepheid work. Solution 1 shows the values of u_o and v_o derived by PMB from radial velocities, and solution 2 shows the results of MCS, also from radial velocities. Solutions 3 and 4 are mean values derived in the present paper from the proper motions in galactic longitude. Solution 3 is a straight mean of the results in Table 5 for solutions 5, 7, 9, 12, 14 and 16. Similarly solution 4 is a straight mean of solutions 2, 4, 7, 9, 10 and 12 in Table 6. These solutions are given primarily to show that the values of u_o and v_o derived from the proper motions do not differ significantly from those obtained from the radial velocities.

The proper motions in galactic latitude can be used to derive a value for the component of the solar motion relative to Cepheids towards the north galactic pole, w_o . This quantity cannot be satisfactorily determined from radial velocities since Cepheids and other young objects lie mainly at low galactic latitude. The equation we have used is,

$$w_o = -\kappa d \mu_b / \cos b + u_o \cos \ell \tan b + v_o \sin \ell \tan b - \frac{R_o}{d} \sin \ell \tan b \left[2A \left(\frac{R_o}{R} - 1 \right) + \frac{(R - R_o)^2}{2R} \Theta_o'' + \frac{(R - R_o)^3}{6R} \Theta_o''' \right]. \quad (16)$$

Since Cepheids are generally close to the galactic plane all of the terms on the right hand side of this equation except the first are small. We have adopted constants from solution 19 of Table 5 with distances from a PLC solution

as in section 3. Table 8 shows the results obtained with the material divided up in various ways. The Cepheids X Cyg (HIP 102276) and RV Sco (HIP 83059) have relatively large residuals from the general solution. Thus solutions omitting them are given. Figure 6 shows the velocity residuals in galactic latitude from solution 1 as seen projected on the Galactic Plane. As with the velocity residuals in the Plane (Fig 5) there is some slight suggestion of a non-random distribution of residuals. There is also some suggestion that the mean residual might be different for stars in the anti-centre direction (positive X) and those with negative X. But the standard errors of solutions 4, 5 and 6 show that any overall difference is hardly significant.

Since there may be some concern that the constraints placed on the rotation curve in the MCS type analyses may affect the derived value of v_o , the best values for the components of the local solar motion from Cepheids are probably the radial velocity values of u_o and v_o from solution 1 of Table 7 and the proper motion solution for w_o (solution 1 of Table 8). These are given as solution 6 in Table 7. For comparison the values for young objects derived by Delhaye (1965) are given as solution 7. It is clear that the modern results remain quite similar to his values.

10 CONCLUSIONS

The following parameters have been derived:

$$\begin{aligned} A &= 14.82 \pm 0.84 \text{ km s}^{-1} \text{ kpc}^{-1}; \\ B &= -12.37 \pm 0.64 \text{ km s}^{-1} \text{ kpc}^{-1}; \\ \Omega_o &= 27.19 \pm 0.87 \text{ km s}^{-1} \text{ kpc}^{-1}; \\ (d\Theta/dR)_o &= -2.4 \pm 1.2 \text{ km s}^{-1} \text{ kpc}^{-1}; \\ u_o &= +9.3 \text{ km s}^{-1} \text{ (adopted from radial velocity solutions);} \end{aligned}$$

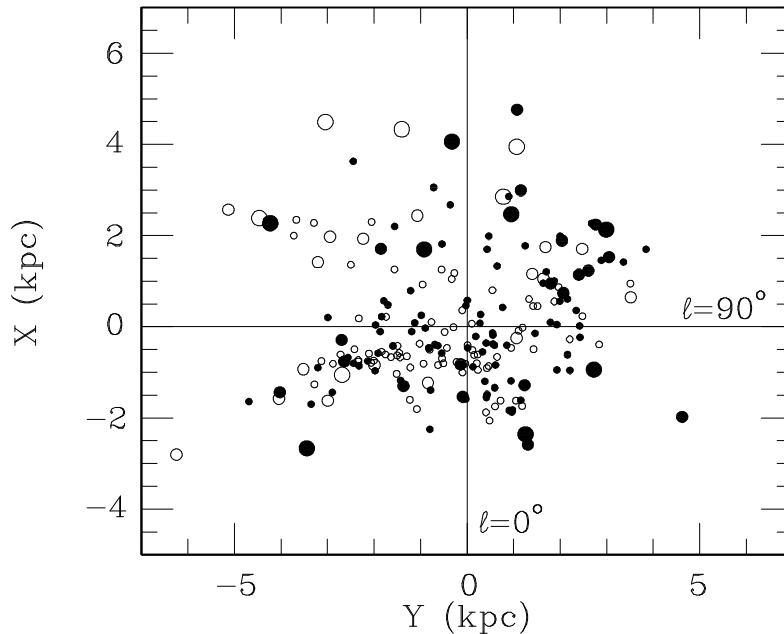


Figure 6. The velocity residuals from the proper motion solution in galactic latitude (solution 1 of Table 8) shown plotted on the galactic plane. Symbols as in Fig 5.

$v_o = +11.2 \text{ km s}^{-1}$ (adopted from radial velocity solutions);

$w_o = +7.61 \pm 0.64 \text{ km s}^{-1}$;

$R_o = 8.5 \pm 0.5 \text{ kpc}$.

The distance scale implied by the comparison of the value of A derived from the proper motions with that derived from radial velocities is found to be in agreement with that derived directly from the Hipparcos trigonometrical parallaxes of the same stars.

Metzger M. R., Caldwell J. A. R., Schechter P. L., 1997, *AJ*, in press (MCS)

Oort J. H., 1927, *Bull. Astr. Inst. Neth.*, 4, 79

Pont F., Mayor M., Burki G., 1994, *A&A*, 285, 415 (PMB)

Pont F., Queloz D., Bratschi P., Mayor M., 1997, *A&A*, 318, 416

Weaver H. F., 1964, in: *The Galaxy and the Magellanic Clouds*, IAU Symp. 20, ed. Kerr F. J., Rodgers A.W., Aust. Acad. Sc. Canberra, p92

Acknowledgements

We are grateful to the Hipparcos team for early access to this remarkable data set, to Metzger et al. for their preprint and to Dr F. Pont and the referee (Prof J. Binney) for some helpful comments.

REFERENCES

- Binney J., Dehnen W., 1997, *MNRAS*, preprint
 Brand J., Blitz L., 1993, *A&A*, 275, 67
 Caldwell J. A. R., Coulson I. M., 1987, *AJ*, 93, 1090
 Delhaye J., in *Galactic Structure*, ed. Blaauw A., Schmidt M., 1965, Chicago University Press, Chicago, p. 61
 ESA 1997, *The Hipparcos Catalogue*, ESA SP-1200
 Feast M. W., 1967, *MNRAS*, 136, 141
 Feast M. W., Walker A. R., 1987, *ARAA*, 25, 345
 Feast M. W., Catchpole R. M., 1997, *MNRAS*, in press (paper 1)
 Fernie J. D., 1990, *ApJS*, 72, 153
 Fernie J. D., Beattie B., Evans N. R., Seager S., 1995, *Inf. Bull. Var. Stars*, No. 4148
 Humphreys R. M., 1972, *A&A*, 20, 29
 Laney C. D., Stobie R. S., 1993, *MNRAS*, 263, 921
 Laney C. D., Stobie R. S., 1994, *MNRAS*, 266, 441
 Martin W. L., Warren P. R., Feast M. W., 1979, *MNRAS*, 188, 139

Table 1: Photometric Data

HIP ID	$\langle V \rangle$	$\langle B \rangle - \langle V \rangle$ (mag)	E_{B-V}	log P	GCVS name	Note
1162	9.127	0.989	0.345	0.764	FM Cas	
1213	9.868	0.992	0.464	0.610	SY Cas	
2085	7.733	0.582	0.115	0.330	TU Cas	
2347	8.969	1.154	0.490	0.903	DL Cas	
3886	9.935	1.147	0.430	0.653	XY Cas	
5138	10.697	1.245	0.475	0.778	VW Cas	
5658	11.338	1.110	0.520	0.629	UZ Cas	
5846	10.920	1.550	0.948	0.797	BP Cas	
7548	9.117	1.096	0.382	1.170	RW Cas	
8312	10.366	1.309	0.796	0.662	BY Cas	o
8614	10.724	1.143	0.553	0.793	VV Cas	
9928	9.312	1.158	0.500	1.037	VX Per	
10332	11.664	1.027	0.538	0.660	UX Per	
11420	9.853	1.419	0.817	1.135	SZ Cas	
11767	1.982	0.598	-0.034	0.754	α UMi	o
12817	10.848	1.181	0.599	0.583	DF Cas	
13367	5.970	0.703	0.204	0.440	SU Cas	o
18260	8.691	1.351	0.590	1.215	RW Cam	
19057	7.682	1.193	0.553	0.898	RX Cam	
19978	11.158	1.155	0.490	0.632	SX Per	
20202	9.723	1.302	0.676	0.697	AS Per	
21517	6.530	0.852	0.274	0.651	SZ Tau	o
22275	7.492	1.055	0.464	0.810	AW Per	
22445	9.020	1.029	0.385	1.046	SV Per	
23210	10.455	1.218	0.593	1.012	AN Aur	
23360	7.655	1.009	0.246	1.065	RX Aur	
24105	9.427	1.062	0.446	0.903	BK Aur	
24281	9.074	1.000	0.407	1.006	SY Aur	
24500	10.332	1.375	0.565	1.260	YZ Aur	
25642	9.607	0.911	0.394	0.587	Y Aur	
26069	3.756	0.799	0.079	0.993	β Dor	
27119	8.217	0.847	0.355	0.606	ST Tau	
28625	10.007	1.025	0.566	0.743	RZ Gem	
28945	9.721	1.061	0.316	1.053	AA Gem	
29022	11.381	0.924	0.402	0.590	CS Ori	
30219	8.219	1.048	0.229	1.183	SV Mon	
30286	8.412	0.945	0.362	0.879	RS Ori	
30541	6.123	1.168	0.172	1.432	T Mon	
30827	5.446	0.595	0.047	0.571	RT Aur	
31404	6.950	0.889	0.251	0.898	W Gem	
31624	10.306	1.337	0.764	0.731	CV Mon	
32180	9.857	0.694	0.113	0.578	AD Gem	
32854	10.960	1.096	0.512	0.940	TX Mon	
33014	11.048	1.195	0.559	0.597	EK Mon	
33520	10.761	1.116	0.404	0.871	TZ Mon	

HIP ID	$\langle V \rangle$	$\langle B \rangle - \langle V \rangle$ (mag)	E_{B-V}	log P	GCVS name	Note
33791	10.067	1.165	0.512	0.904	AC Mon	
34088	3.918	0.798	0.080	1.006	ζ Gem	
34527	10.582	1.175	0.577	0.669	TV CMa	
35212	8.110	0.847	0.236	0.670	RY CMa	
35665	9.697	1.004	0.456	0.629	RZ CMa	
35708	9.561	0.970	0.334	0.845	TW CMa	
36088	9.915	1.212	0.566	1.092	SS CMa	
36617	11.365	1.065	0.475	0.632	VW Pup	
36666	8.328	0.610	0.165	0.479	VX Pup	
36685	8.507	1.208	0.417	1.414	X Pup	
37207	9.631	1.158	0.478	1.365	VZ Pup	
37511	10.554	0.874	0.388	0.742	WW Pup	
37515	9.063	0.968	0.310	0.951	WX Pup	
38063	9.863	1.049	0.341	1.133	AD Pup	
38907	7.371	0.838	0.232	0.706	AP Pup	
38944	10.569	0.791	0.273	0.720	WY Pup	
38965	8.669	1.337	0.555	1.479	AQ Pup	
39144	10.326	0.789	0.203	0.701	WZ Pup	
40155	5.695	0.579	0.060	0.782	AH Vel	o
40178	7.957	0.783	0.223	0.824	AT Pup	
40233	7.028	1.434	0.484	1.617	RS Pup	
41588	7.375	0.870	0.191	0.826	V Car	
42257	7.089	1.129	0.296	1.310	RZ Vel	
42321	8.032	0.934	0.284	0.667	T Vel	
42492	10.017	0.991	0.510	0.495	AP Vel	
42831	8.121	1.151	0.356	1.370	SW Vel	
42926	8.277	0.885	0.276	0.980	SX Vel	
42929	9.704	1.195	0.520	0.768	ST Vel	
44847	7.635	1.175	0.450	0.840	BG Vel	
45949	7.589	0.788	0.149	0.641	V Vel	
46746	9.520	1.518	0.682	1.049	DR Vel	
47177	10.262	1.243	0.646	0.853	AE Vel	
47854	3.735	1.260	0.194	1.551	l Car	
48663	9.364	1.043	0.388	0.857	GX Car	
50244	10.700	1.089	0.410	0.693	CN Car	
50615	10.261	0.979	0.443	0.619	GZ Car	
50655	8.372	1.367	0.558	1.449	RY Vel	
50722	8.851	0.928	0.182	0.990	AQ Car	
51142	9.426	0.971	0.478	0.728	UW Car	
51262	8.714	1.124	0.398	1.259	YZ Car	
51338	8.308	0.627	0.126	0.566	UX Car	
51653	8.084	0.585	0.126	0.561	Y Car	
51894	10.654	1.162	0.530	0.844	XX Vel	
51909	9.323	0.875	0.206	0.716	UZ Car	
52380	10.318	0.854	0.352	0.459	EY Car	

HIP ID	$\langle V \rangle$	$\langle B \rangle - \langle V \rangle$ (mag)	E_{B-V}	log P	GCVS name	Note
52538	7.460	1.164	0.230	1.279	VY Car	
52570	8.524	1.054	0.407	1.149	SV Vel	
52661	9.089	0.887	0.344	0.687	SX Car	
53083	9.743	0.890	0.427	0.670	WW Car	
53397	9.255	1.149	0.384	1.362	WZ Car	
53536	9.322	1.054	0.362	1.196	XX Car	
53589	6.281	1.178	0.277	1.588	U Car	
53593	9.782	0.953	0.389	0.630	CY Car	
53867	11.542	1.101	0.578	0.661	FN Car	
53945	9.295	1.214	0.420	1.095	XY Car	
54101	8.601	1.266	0.371	1.221	XZ Car	
54543	6.824	0.867	0.110	0.888	ER Car	
54621	9.177	0.932	0.385	0.758	GH Car	
54715	8.097	0.990	0.279	0.877	IT Car	
54862	8.323	0.739	0.195	0.802	GI Car	o
54891	9.661	1.121	0.337	1.030	FR Car	
55726	8.830	1.009	0.320	0.725	AY Cen	
55736	8.636	0.653	0.177	0.660	AZ Cen	o
56176	8.186	0.758	0.183	0.741	V419 Cen	
56991	8.765	0.740	0.255	0.523	UZ Cen	
57130	11.480	1.282	0.596	1.086	KK Cen	
57260	9.022	0.834	0.382	0.489	RT Mus	
57649	10.008	0.886	0.371	0.502	BK Cen	
57884	9.783	1.147	0.411	1.066	UU Mus	
57978	10.073	0.953	0.389	0.757	BB Cen	o
59551	6.127	0.831	0.268	0.985	S Mus	
59575	11.051	1.279	0.677	0.806	AD Cru	
59996	9.796	1.752	1.051	1.109	SU Cru	
60259	6.566	0.922	0.178	0.828	T Cru	
60455	6.766	0.772	0.167	0.765	R Cru	
61981	6.298	0.757	0.132	0.876	R Mus	
62986	6.600	0.761	0.167	0.671	S Cru	
63693	9.966	1.172	0.574	0.646	V496 Cen	
64969	8.460	1.035	0.398	0.810	V378 Cen	
66189	10.242	1.347	0.418	1.177	VW Cen	
66383	9.855	1.622	0.751	1.532	KN Cen	
66696	7.818	0.982	0.275	1.040	XX Cen	
67566	7.653	0.792	0.213	0.706	V381 Cen	
70203	8.753	1.191	0.419	0.976	V339 Cen	
71116	6.823	0.872	0.302	0.740	V Cen	
72773	5.880	0.741	0.371	0.722	AX Cir	
74448	9.566	1.314	0.596	0.916	IQ Nor	
75018	6.660	0.722	0.164	0.530	R TrA	
76918	9.229	1.622	0.921	1.102	U Nor	
77913	9.513	1.340	0.646	1.102	SY Nor	

HIP ID	$\langle V \rangle$	$\langle B \rangle - \langle V \rangle$ (mag)	E_{B-V}	log P	GCVS name	Note
78476	6.397	0.752	0.092	0.801	S TrA	
78771	11.670	2.000	1.194	1.033	TW Nor	
78797	10.027	1.287	0.552	0.792	RS Nor	
78978	7.878	0.608	0.104	0.410	U TrA	
79625	10.411	1.273	0.684	0.538	GU Nor	
79932	6.426	0.945	0.196	0.989	S Nor	
82498	9.810	1.936	0.886	1.458	KQ Sco	
83059	7.040	0.955	0.366	0.783	RV Sco	
83674	7.332	0.856	0.268	0.609	BF Oph	
85035	6.654	0.936	0.211	0.832	V636 Sco	
85701	7.965	0.975	0.335	0.656	V482 Sco	
87072	4.549	0.739	0.240	0.846	X Sgr	
87173	8.729	1.276	0.608	0.969	V500 Sco	
87345	8.016	1.480	0.702	1.308	RY Sco	
87495	6.150	1.385	0.630	1.234	Y Oph	
88567	4.668	0.746	0.119	0.881	W Sgr	
89013	10.842	1.644	1.011	0.724	CR Ser	
89276	6.955	0.807	0.165	0.704	AP Sgr	
89596	8.023	1.404	0.438	1.339	WZ Sgr	
89968	5.744	0.856	0.179	0.761	Y Sgr	
90110	10.549	1.457	0.822	0.818	AY Sgr	
90241	8.852	1.107	0.525	0.808	XX Sgr	
90791	10.006	1.140	0.654	0.623	X Sct	
90836	6.685	1.091	0.412	0.829	U Sgr	
91239	10.131	1.182	0.664	0.490	EV Sct	
91366	9.628	1.539	0.765	1.015	Y Sct	
91613	10.590	1.566	0.820	0.870	CK Sct	
91697	9.465	1.701	0.965	1.294	RU Sct	
91706	10.831	1.657	0.939	1.043	TY Sct	
91738	11.106	1.371	0.737	0.593	CM Sct	
91785	9.600	1.330	0.485	1.111	Z Sct	
91867	8.211	0.944	0.329	0.565	SS Sct	
92013	7.483	0.905	0.284	0.712	V350 Sgr	
92370	7.358	1.032	0.292	0.980	YZ Sgr	
92491	6.932	0.985	0.295	0.822	BB Sgr	
93063	11.083	1.280	0.684	0.475	V493 Aql	
93124	5.372	0.756	0.173	0.806	FF Aql	o
93399	9.848	1.312	0.608	0.864	V336 Aql	
93681	8.617	1.429	0.540	1.234	SZ Aql	
93990	7.141	1.292	0.444	1.138	TT Aql	
94004	7.751	1.146	0.395	0.833	V496 Aql	
94094	8.270	1.277	0.629	0.786	FM Aql	
94402	8.382	1.214	0.503	0.977	FN Aql	
95118	10.037	1.462	0.834	0.860	V600 Aql	
95820	6.446	1.024	0.341	0.847	U Aql	

HIP ID	$\langle V \rangle$	$\langle B \rangle - \langle V \rangle$ (mag)	E_{B-V}	$\log P_0$	GCVS name	Note
96458	7.128	1.275	0.654	0.903	U Vul	
96596	10.710	0.847	0.229	0.746	V924 Cyg	
97150	6.859	0.575	0.077	0.585	SU Cyg	
97717	7.243	1.465	0.431	1.653	SV Vul	
97804	3.897	0.789	0.146	0.856	η Aql	
98085	5.622	0.805	0.092	0.923	S Sge	
98212	8.849	1.389	0.709	0.801	X Vul	
98376	9.924	1.266	0.662	0.893	GH Cyg	
98852	8.947	1.266	0.487	1.232	CD Cyg	
99276	9.873	1.008	0.376	0.640	V402 Cyg	
99567	9.489	1.316	0.633	0.775	MW Cyg	
101393	9.432	1.477	0.570	1.179	SZ Cyg	
102276	6.391	1.130	0.223	1.214	X Cyg	
102949	5.754	0.635	0.039	0.647	T Vul	
103433	10.069	1.704	0.791	1.304	VX Cyg	
103656	9.511	1.784	1.151	1.168	TX Cyg	
104002	9.593	1.215	0.633	0.895	VY Cyg	
104185	5.774	0.538	0.004	0.549	DT Cyg	o
104564	10.601	1.439	0.763	0.860	V459 Cyg	
104877	9.635	1.491	0.854	0.721	V386 Cyg	
105369	9.086	1.036	0.455	0.516	V532 Cyg	
106754	10.456	1.283	0.675	0.787	V538 Cyg	
107899	8.959	0.876	0.246	0.687	VZ Cyg	
108427	10.590	1.668	0.682	1.252	CP Cep	
108630	8.883	0.949	0.304	0.727	BG Lac	
109340	9.146	0.731	0.170	0.636	Y Lac	
110964	11.180	1.341	0.704	0.859	AK Cep	
110991	3.954	0.657	0.089	0.730	δ Cep	
111972	8.415	1.095	0.339	1.037	Z Lac	
112026	8.848	0.885	0.287	0.807	RR Lac	
112430	9.656	1.396	0.720	0.795	CR Cep	
112626	8.936	0.873	0.286	0.698	V Lac	
112675	8.407	0.901	0.296	0.736	X Lac	
114160	9.705	1.081	0.457	0.736	SW Cas	
115390	10.973	1.650	0.939	1.179	CM Cas	
115925	11.641	1.738	0.986	1.158	CY Cas	
116556	9.932	1.490	0.875	0.799	RS Cas	
116684	11.112	1.475	0.884	0.699	DW Cas	
117154	10.738	1.449	0.818	0.892	CD Cas	
117690	9.927	1.384	0.649	1.084	RY Cas	
118122	9.876	1.188	0.464	0.992	DD Cas	
118174	11.136	1.174	0.523	0.688	CF Cas	

Table 2: Zero-point of $\langle M_V \rangle = -2.87 \log P + \rho_1$

Solution	N	Description	ρ_1	Weight
1	220	Whole Sample	-1.36 ± 0.11	1854
2	219	Whole Sample minus α UMi	-1.35 ± 0.15	982
3	25	High Weight minus α UMi	-1.39 ± 0.13	794
4	26	High Weight plus α UMi	-1.38 ± 0.09	1613

Table 3: Zero-point of $\langle M_V \rangle = -3.80 \log P + 2.70(\langle B \rangle - \langle V \rangle)_0 + \rho_2$

Solution	N	$\sigma_{PLC} = 0$	Weight	$\sigma_{PLC} = 0.10$	$\sigma_{PLC} = 0.20$
		ρ_2		ρ_2	ρ_2
1	220	-2.35 ± 0.11	4671	-2.36 ± 0.12	-2.37 ± 0.14
2	219	-2.35 ± 0.15	2498	-2.36 ± 0.15	-2.37 ± 0.16
3	25	-2.40 ± 0.13	1885	-2.41 ± 0.13	-2.42 ± 0.14
4	26	-2.38 ± 0.09	4061	-2.38 ± 0.10	-2.40 ± 0.11

Table 4: First order (Oort-type) solutions

Solution	N	u_o (km s ⁻¹)	v_o (km s ⁻¹)	A (km s ⁻¹ kpc ⁻¹)	Ω_o (km s ⁻¹ kpc ⁻¹)	Remarks
1	214	9	13	15.20±0.88	27.31±0.88	
2	214	9.32	11.18	15.05±0.88	27.31±0.88	$B = -12.26 \pm 0.64$
3	214	9.32	11.18	15.02±0.89	27.28±0.89	PLC distances
4	214	9.32	11.18	15.03±0.88	27.05±0.88	$\Delta m = 0.4$
5	109	9.32	11.18	14.76±1.35	27.80±1.59	$d \cos b < 2$ kpc
6	105	9.32	11.18	15.62±1.21	27.23±1.06	$d \cos b \geq 2$ kpc
7	214	9.32	11.18		26.69±0.83	$2A = \Omega_0$

Table 5: PMB-type solutions

Solution	u_o (km s ⁻¹)	v_o	R_o (kpc)	Θ_o''	Θ_o''' (km s ⁻¹ kpc ⁻¹)	A	Ω_o	Remarks
(a) Radial Velocity Solutions								
1	9.32±0.80	11.18±0.65	8.09±0.30	-3.38±0.38	+1.99±0.62	15.92±0.34		*
2			8.9	-2.85	+1.60			$\Delta\rho_2 = -0.20$
(b) Proper Motion Solutions (PL Distances)								
3	9.05±1.49	16.60±2.13	8.09(set)	+5.52±2.28	-0.89 ± 2.14	15.70±1.10	26.85±0.90	
4	9.32(set)	11.18(set)	8.09(set)	+1.60±1.68	+1.13 ± 1.99	15.70±1.08	27.29±0.86	
5	9.83±1.48	9.88±1.50	8.09(set)	-3.38(set)	+1.99(set)	14.78±0.85	27.27±0.89	
6	9.32(set)	11.18(set)	8.09(set)	-3.38(set)	+1.99(set)	14.81±0.83	27.24±0.86	
7	9.87±1.48	10.53±1.50	8.90(set)	-2.85(set)	+1.60(set)	14.79±0.85	27.21±0.89	
8	9.32(set)	11.18(set)	8.90(set)	-2.85(set)	+1.60(set)	14.84±0.84	27.23±0.86	
9	9.68±1.48	12.46 ±1.50	8.90(set)	0 (set)	0 (set)	14.75±0.85	27.05±0.89	
10	9.32(set)	11.18(set)	8.90(set)	0 (set)	0 (set)	14.80±0.84	27.19±0.86	
11	10.01±1.47	12.27±1.50	8.90(set)	0 (set)	0 (set)	13.27±0.43	2A (set)	
12	9.61±1.48	12.14±1.50	8.09(set)	0 (set)	0 (set)	14.70±0.85	27.07±0.89	
13	9.32(set)	11.18(set)	8.09(set)	0 (set)	0 (set)	14.75±0.83	27.19±0.86	
(c) Proper Motion Solutions (PLC Distances)								
14	9.77±1.48	9.88±1.50	8.09(set)	-3.38(set)	+1.99(set)	14.75±0.86	27.23±0.90	
15	9.32(set)	11.18(set)	8.09(set)	-3.38(set)	+1.99(set)	14.78±0.84	27.19±0.87	
16	9.81±1.48	10.52±1.50	8.90(set)	-2.85(set)	+1.60(set)	14.77±0.86	27.17±0.90	
17	9.32(set)	11.18(set)	8.90(set)	-2.85(set)	+1.60(set)	14.81±0.84	27.19±0.87	
18	9.32(set)	11.18(set)	8.90(set)	-2.85(set)	+1.60(set)	14.63±1.02	26.80±1.04	$\Delta\rho_2 = +0.4$
19	9.32(set)	11.18(set)	8.50(set)	-3.11(set)	+1.83(set)	14.82±0.84	27.19±0.87	$B = -12.37 \pm 0.64$

* Solution 1: internal errors only (see text section 6).

Table 6: MCS-type solutions

Solution	u_o (km s ⁻¹)	v_o	R_o (kpc)	A (km s ⁻¹ kpc ⁻¹)	Ω_o	f (km s ⁻¹)
(a) Radial Velocity Solution						
1	9.3±1.1	13.5±1.0	7.66±0.54	15.47±1.2		+10.2±3.8
(b) Proper Motion Solutions						
2	9.74±1.57	11.77±1.51	7.66(set)		26.61±0.86	-1.21±4.37
3	9.32(set)	11.18(set)	7.66(set)		26.70±0.83	-1.78±4.08
4	9.89±1.47	11.82±1.50	7.66(set)		26.62±0.85	0 (set)
5	9.3(set)	13.5(set)	7.66(set)		26.51±0.83	-1.14±4.08
6	9.3(set)	13.5(set)	7.66(set)		26.80±0.83	+10.2(set)
7	9.79±1.56	11.94±1.51	8.09(set)		26.58±0.85	-1.33±4.64
8	9.32(set)	11.18(set)	8.09(set)		26.69±0.83	-2.01±4.36
9	9.94±1.47	11.99±1.50	8.09(set)		26.59±0.85	0 (set)
10	9.87±1.54	12.22±1.51	8.90(set)		26.54±0.85	-1.56±5.16
11	9.32(set)	11.18(set)	8.90(set)		26.68±0.83	-2.45±4.90
12	10.01±1.47	12.27±1.50	8.90(set)		26.54±0.85	0 (set)

Table 7: Solar Motion

Solution	u_o	v_o (km s^{-1})	w_o	Remarks
1	9.3 ± 0.80	11.18 ± 0.65		PMB
2	9.3 ± 1.1	13.5 ± 1.0		MCS
3	9.76 ± 1.48	10.90 ± 1.50		PM(PMB-type)
4	9.87 ± 1.51	12.00 ± 1.50		PM(MCS-type)
5			7.61 ± 0.64	PM
6	9.3	11.2	7.6	Suggested Best
7	9	12	7	Delhaye

Table 8: w_o Solutions

Solution	w_o (km s ⁻¹)	N	Remarks
1	7.61±0.64	214	
2	7.88±0.64	213	Omits X Cyg
3	7.67±0.65	212	Omits X Cyg and RV Sco
4	8.82±1.16	90	X > 0
5	7.08±0.77	124	X < 0
6	7.46±0.77	123	X < 0, omits X Cyg